The Planetary Science Journal, 4:55 (15pp), 2023 March https://doi.org/10.3847/PSJ/acc337

Influences on Infrared Spectra of Benzene Ices for Titan, Comets, and Beyond: Annealings, Artifacts, and Isosbestic Points

Reggie L. Hudson and Perry A. Gerakines
Astrochemistry Laboratory, NASA Goddard Space Flight Center, Greenbelt, MD 20771 USA; reggie.hudson@nasa.gov
Received 2022 July 16; revised 2023 February 5; accepted 2023 February 17; published 2023 March 31

Abstract

Infrared (IR) spectra are needed for both laboratory and observational studies of extraterrestrial ices, both within the solar system, such as for trans-Neptunian objects, comets, and Titan, and in the interstellar medium. Here we present new transmission-IR measurements on solid benzene (C_6H_6), the simplest common aromatic compound. Spectra are shown with a greater combination of higher resolutions and temperatures than found in the literature. The influences of both warmings and annealings on amorphous benzene are described, and comparisons are made of the IR spectra of warmed and cooled crystalline benzene. Reversible variations with temperature are noted for several IR bands of crystalline benzene, with a suggestion for their use as a possible thermometer for remote sensing of extraterrestrial environments. Comparisons are made to both recent and older literature results, and an artifact produced by high vapor-phase condensation rates is identified. New density measurements are reported for crystalline benzene and used, along with IR-forbidden transitions, to identify amorphous and crystalline ices. It is suggested that differences in spectra of crystalline benzene ices at the same temperature do not necessarily imply partial crystallization.

Unified Astronomy Thesaurus concepts: Titan (2186); Comets (280); Molecular spectroscopy (2095); Laboratory astrophysics (2004); Astrochemistry (75); Small molecules (2267); Ice spectroscopy (2250); Interstellar molecules (849)

1. Introduction

Infrared (IR) spectroscopy has been and remains the primary tool for the identification and quantification of ices in extraterrestrial environments. Remote-sensing applications include usage with such high-profile instrumentation and observatories as the Infrared Space Observatory, the Spitzer Space Telescope, the Stratospheric Observatory for Infrared Astronomy (SOFIA), the Kuiper Airborne Observatory (KAO), the Hubble Space Telescope, and the James Webb Space Telescope (JWST).. The data returned from such instruments and projects often rely on low-temperature laboratory measurements for interpretation and quantification. Our research group has been involved in generating such reference data for several decades, as well as investigating chemical changes in and physical properties of ices in the interstellar medium (ISM), comets, icy satellites, and on Mars. Here we examine the IR spectra of benzene (C_6H_6) at temperatures relevant for interstellar ices, comets, trans-Neptunian objects (TNOs), and, in particular, Titan's atmosphere.

Benzene is the simplest common aromatic compound, each benzene molecule consisting of a regular planar hexagonal arrangement of carbon atoms, with each carbon bonded to a single hydrogen atom. Benzene has been detected in the ISM (Cernicharo et al. 2001), in Comet 67P (Schuhmann et al. 2019), and in the atmospheres of Jupiter and Saturn (Bézard et al. 2001). Benzene is a precursor to more complex polycyclic aromatic hydrocarbons of the ISM (Cherchneff 2011, and references therein). Chemical derivatives of benzene have been identified in meteorites (e.g., Sephton 2002), and benzene ice has been identified on Titan by Coustenis et al. (2003), with subsequent studies by others (Vinatier et al. 2018).

According to the Harvard ADS database, since 2020 January 1 at least a dozen refereed papers have appeared on benzene in the astrophysical, astrochemical, and astrobiological literature, covering the compound's extraterrestrial synthesis, physical properties, and chemical reactions. Of particular interest here are two recent planetary-science papers presenting mid-IR spectra of solid benzene. Mouzay et al. (2021) reported spectra of benzene ices obtained by condensation of benzene vapor onto a gold-coated surface at 16 K. Spectra reflected from the ice and substrate were presented at a resolution of 1 cm^{-1} at 16 to 130 K, with the amorphous and crystalline forms of the solid being clearly identified. In a separate study, Nna-Mvondo & Anderson (2022) condensed C_6H_6 onto a diamond substrate at 12 temperatures from 15 to 130 K, with transmission spectra being recorded at 4 cm^{-1} resolution, but with no spectra shown for ices that were subsequently warmed or cooled.

These same two papers reported new results, but additional work on solid benzene remains to be done. For example, the IR-reflection arrangement adopted by Mouzay et al. (2021) characterized the form of the authors' benzene ices, but the relative intensities of the spectral features shown do not match those in a transmission spectrum, and the band intensities and peak heights do not vary linearly with sample thickness or IR path length through the ice sample. Neither the ice sample's thickness nor the angle of the incident IR beam with respect to the gold-coated substrate were stated, making quantitative reproduction of the authors' work difficult. IR spectra recorded in a conventional transmission mode for benzene ices of known thickness and over a range of temperatures are still needed.

Nna-Mvondo & Anderson (2022) presented new IR transmission spectra of benzene ices, but their spectral resolution of only 4 cm^{-1} is much less than the 0.5 cm^{-1}

found in papers from the 1960s (e.g., Anderson & Person 1962; Hollenberg & Dows 1962; Hollenberg & Glover 1967; Glover & Hollenberg 1969). Moreover, many figures were presented with 12 spectra superimposed and with the 12 ice samples having different thicknesses, making it difficult to examine individual spectra and extract trends. Also, the IR spectra shown are for ices made at different temperatures, but without any subsequent warming or cooling to reveal and document any possible temperature-dependent IR features. For example, differences are clearly seen in the authors' IR spectra shown for benzene ices made, and with spectra recorded, at 60 and 100 K, but it is not known if such differences would remain if the ices were brought to the same temperature following their formation. Such measurements and comparisons are still needed.

Our group's interest in extraterrestrial benzene ices has covered the compound's radiation chemistry and radiolytic stability, its vapor pressures, densities, and refractive indices, and solid benzene's IR spectra, including IR intensity measurements and optical constants (e.g., Ruiterkamp et al. 2005; Callahan et al. 2013; Hudson & Yarnall 2022; Hudson et al. 2022a). Having addressed quantitative aspects of the IR spectra of benzene ices, we now examine influences on and interpretations of them. For amorphous benzene, we focus on temperatures under about 50 K, which are relevant for ices of interstellar grains, comets, and TNOs, and for crystalline benzene we concentrate on temperatures at and above 100 K, for applications to Titan and a few other icy satellites. We also report new results on the amorphous-to-crystalline conversion. Of more general interest is how the IR spectra of amorphous and crystalline benzene and other compounds can depend on the conditions of ice growth, post-growth thermal history, and spectral measurement. Viewed this way, the present paper links and expands on those of Mouzay et al. (2021), who reported reflection-IR spectra of benzene ices after growth followed by warmings and coolings, and the study of Nna-Mvondo & Anderson (2022), who published transmission-IR spectra for ices grown at multiple temperatures, but no subsequent temperature changes for the samples.

2. Experimental Methods

The equipment used and procedures followed were almost entirely those described in our recent papers (e.g., Hudson et al. 2017; Gerakines et al. 2022), so only a summary and a few comments are needed here.

Ices were made by vapor-phase condensation of benzene vapor onto a cesium iodide (CsI) substrate precooled to the temperature of interest (10–150 K) in a vacuum system ($\sim 10^{-8}$ Torr at room temperature). Our standard condensation rates gave an increase in the resulting ice's thickness of 1–3 μm hr^{-1} as measured by interferometry (Hollenberg & Dows 1961; Groner et al. 1973). However, in some cases a higher or lower value was adopted to examine the influence of deposition rate on the resulting ice's spectrum. The refractive indices needed to measure ice thicknesses and deposition rates were determined with two-laser interferometry (Tempelmeyer & Mills 1968) under ultra-high vacuum conditions ($\sim 10^{-10}$ Torr); see Hudson et al. (2017) for details. Ice thicknesses ranged from about 0.1 to 4 μm, but mostly were near 0.5 to 1 μm. This choice of thicknesses was influenced by the work of Barth (2017) on the size of benzene ices in Titan's atmosphere and by our desire to study benzene ices comparable in size to those described in the literature (e.g., Anderson & Person 1962; Hollenberg & Dows 1962).

Spectra were recorded with a Thermo iS50 IR spectrometer operating at 6500–400 cm^{-1}, but our interest was primarily in the 4000–500 cm^{-1} (2.5–20 μm) region. Spectral resolutions usually were 0.5 and 1 cm^{-1}, mainly the former for crystalline ices and the latter for amorphous ones. These resolutions were varied in some cases for comparisons to earlier work. Each IR spectrum shown is, with few exceptions, the result of 200 accumulations measured in a standard transmission mode with the incident IR beam perpendicular to the plane of the ice and the CsI substrate. We emphasize that checks were made to ensure that IR features were neither saturated nor resolution limited. Heating rates for ices varied from about 0.5–10 K minute^{-1}, but typically were 1–5 K minute^{-1}. Variations within the 0.5–10 K minute^{-1} range did not influence the resulting spectra.

We refer to benzene ices that were either made at or warmed above about 40 K as crystalline, but more accurately they can be described as polycrystalline. No implication of any sample being a single crystal with or without a particular orientation is intended. We recorded transmission-IR spectra of several of our crystalline-benzene samples at angles up to 30° with respect to a line drawn perpendicular to the substrate. No new features appeared and none that already were present changed, except for slight increases in intensity due to a longer path length through the ice.

Reagent-grade benzene (purity $\geqslant$99%) was purchased from Sigma Aldrich, now MilliporeSigma, and used as received aside from degassing with liquid nitrogen.

3. Results

There were multiple variables to consider for the measurements we undertook. Ice thickness and spectral resolution were important, and tests and checks of each were made in Hudson & Yarnall (2022) and for the present work. An ice's IR spectrum can be influenced by the temperature at which the spectrum is recorded. Examples are in the next sections. Also relevant are the conditions under which an ice is made by vapor-phase condensation, such as the condensation (deposition) temperature and the resulting ice sample's growth rate. It also is important to recognize that an ice's thermal history of warming, cooling, or annealing can influence its IR spectrum. This point was emphasized by Nna-Mvondo & Anderson (2022), but with the statement that studies of crystalline ices made by direct deposition at a temperature of interest "are almost nonexistent" compared to studies of crystalline ices made by warming from a lower temperature. However, we note that there are many publications spanning many years that involve condensations at a specific temperature to make a crystalline solid. See, for example, Hornig et al. (1958), Bertie et al. (1969), Wood & Roux (1982), Baratta et al. (1991), Smith et al. (1994), Garozzo et al. (2008), Satorre et al. (2017), and Luna et al. (2018), as well as work from our own group (e.g., Moore et al. 2007; Yarnall et al. 2020; Gerakines et al. 2022; Hudson et al. 2022b). The method adopted for growing a crystalline ice for spectroscopic study is a well- and long-recognized variable in the type of work presented here.

Benzene is somewhat unusual in aiding the solid-phase IR spectroscopist in a way not possible with most other extraterrestrial compounds. The benzene molecule's center of symmetry, multiple mirror planes, six-fold rotational axis

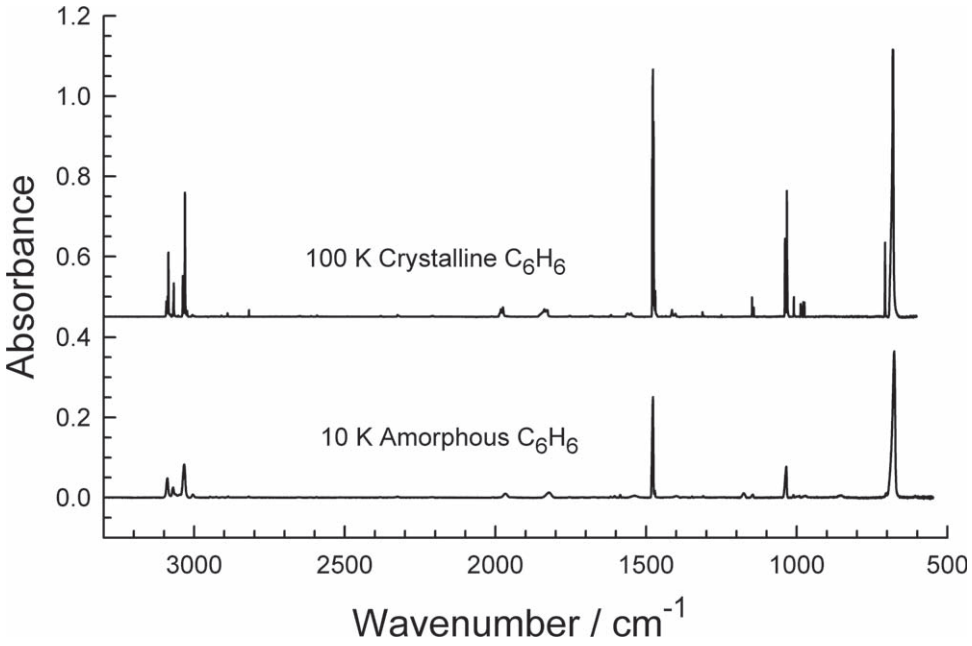

Figure 1. Survey spectra of amorphous and crystalline benzene (C_6H_6). Ices were grown and their spectra recorded with a resolution of 0.5 cm^{-1} at the temperatures indicated. The thicknesses of the amorphous and crystalline ices were about 0.96 and 0.83 μm, respectively, each ice being grown at about 1 μm hr^{-1}. Spectra are offset for clarity. See the text and Hudson & Yarnall (2022) for details.

(i.e., C_6), and six two-fold (i.e., C_2) axes perpendicular to it lead to several vibrational modes being IR-forbidden in the isolated molecule and in the crystalline solid, but not in either the liquid or amorphous-solid forms. In this way, C_6H_6 joins other compounds whose amorphous and crystalline forms and IR spectra we have investigated, namely C_2H_2, C_2H_4, C_2H_6, CH_4, and CO_2 (Hudson et al. 2014a, 2014b; Gerakines & Hudson 2015a, 2015b). Another such molecule studied (Moore et al. 2010) is cyanogen, C_2N_2, found in Titan's atmosphere (e.g., Kunde et al. 1981; Teanby et al. 2009). Each of these seven molecules has at least one nominally IR-forbidden feature that can serve as a tracer of its amorphous-solid form independent of other knowledge of an ice sample's history. Such forbidden transitions were valuable tracers of amorphous benzene in our ices, the absence of such features indicating that a sample had crystallized.

In what follows, we first report measurements of two physical properties of our ices; we then examine IR spectra of ices below ~50 K, then ices above ~50 K; and, finally, the crystallization of amorphous benzene. Most of our work involves variations of temperature and deposition rate on an ice's spectrum. We usually refer to absorbance features in our spectra by their positions (i.e., wavenumber) as opposed to a spectroscopic symbol. Where the latter are used, we have followed the convention of the International Union of Pure and Applied Physics as described by Mulliken (1955, 1956) as opposed to Herzberg's convention. Differences in the two systems arise mainly from the choices for the six C_2 rotational axes in the plane of benzene's six carbon atoms; see Table 6 of Bertie & Keefe (2004) or page 363 of Herzberg (1945) for a comparison.

3.1. Two Physical Properties

In comparing the results on different ices, it was necessary to know the thickness of each sample. Ice thicknesses were determined by two-laser interferometry, which required reference refractive indices for solid benzene. These were measured at a wavelength of 670 nm, and so are designated n_{670}; see our earlier papers for details on the measurements, including equipment and procedures (e.g., Hudson et al. 2017; Gerakines et al. 2022). The values we measured for amorphous benzene at 10 K and crystalline benzene at 100 K were 1.402 and 1.620, respectively, as reported in Hudson & Yarnall (2022). The 1.402 value also was used for amorphous ices grown at temperatures up to 45 K, given that only small changes were seen in their IR spectra with temperature (Section 3.2). A few ices were grown at 130 K, so we measured the refractive index of crystalline benzene there too, finding $n_{670} = 1.610$. These values are averages of triplicate measurements (or more), with uncertainties of about ± 0.005 (standard error).

As a byproduct of our refractive index determinations, we also measured the densities (ρ) of crystalline benzene at three temperatures with our microbalance system. We found $\rho = 1.09$, 1.08, and 1.07 g cm^{-3} at 70, 100, and 130 K, respectively (± 0.005 g cm^{-3}). These densities for ices made by vapor-phase deposition are only about 1% different (smaller) than those from diffraction measurements on polycrystalline benzene (Fortes & Capelli 2018), with both sets of results showing a small density decrease on going from 70 to 100 to 130 K.

3.2. Amorphous C_6H_6 Ices at T $\leqslant$ ~50 K

Transmission-IR spectra of amorphous and crystalline C_6H_6 ices near 10 and 100 K, respectively, were presented in Hudson & Yarnall (2022). Figure 1 shows survey spectra similar to those published there. Our focus in the present paper is on the four regions of greatest IR intensity between 3500 and 500 cm^{-1}, near 3050, 1480, 1035, and 680 cm^{-1}. Table 1 gives approximate descriptions of the vibrational motions associated with these four regions.

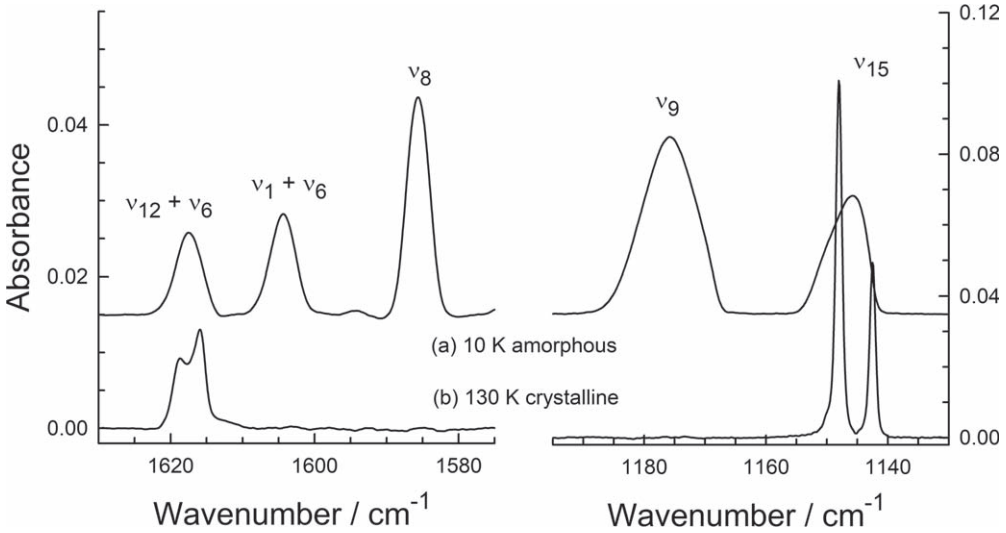

Figure 2. Spectra of amorphous and crystalline benzene at 1 cm^{-1} resolution showing the loss of three forbidden transitions as the ice crystallized on warming from 10 to 130 K. The amorphous ice had a thickness of ~4.8 μm, was grown at ~3 μm hr^{-1}, and was made and its spectrum recorded at 10 K before warming to 130 K. Spectra are offset vertically for clarity.

We also recognize that weaker features, including overtone, combination, and difference bands, can be seen in Figure 1. Several small features were observed (e.g., near 1604, 1586, 1347, 1177, and 853 cm^{-1}) that correspond to IR transitions that are allowed in liquid and amorphous benzene but not in the gas or crystalline phases (e.g., see Mair & Hornig 1949). Figure 2 shows an example of three such IR bands that were lost when an amorphous ice was warmed.

Figure 3 shows expansions of our four regions of interest for amorphous benzene from Table 1. The spectra are of an ice made by vapor-phase condensation at 10 K, followed by warming to 20, 30, 40, and 50 K. It is readily seen that the spectra hardly changed with temperature. However, when we warmed amorphous benzene from 10 K to 50–60 K and either held there or warmed slightly higher, the ice crystallized. In this we were anticipated by Ishii et al. (1996) using both Raman spectroscopy and powder X-ray diffraction. Those authors reported that when amorphous benzene crystallized, (i) the broad diffraction pattern of the sample was replaced by several sharp diffraction spikes, and (ii) sharper Raman peaks appeared at the expense of broad structure-less bands. Ishii et al. (1996) also found that crystallization could be initiated by growth of an ice by vapor-phase deposition at temperatures slightly under 50 K, an observation we return to later. A third independent report of crystallization in the 50–60 K region comes from the study of Mouzay et al. (2021).

In contrast to this 50–60 K region for crystallization of micrometer-sized amorphous-benzene ices, Jakob & Menzel (1996) reported that the amorphous-to-crystalline change first occurred at increasingly higher temperatures as thinner ices were examined. For example, crystallization was first seen near 90 K on warming (0.1 K s^{-1}) an amorphous-benzene ice of about 5 monolayers (MLs) in coverage, near 80 K for a 7 ML ice, and slightly under 60 K for a 15 ML ice. The smallest amorphous-benzene ice for which we felt confident in measuring a size had a thickness of 0.1 μm, for which we calculated a column density of 6×10^{16} molecules cm^{-2} and a coverage of 400 MLs. Not surprisingly, this ice was seen to crystallize near 55 K. (For this calculation we used the conversion factor of Yuan et al. (2013), with 1 ML of coverage corresponding to about 1.5×10^{14} molecules cm^{-2} of column density.) For evidence of crystallization near 40 K, see also the benzene-desorption work of May et al. (2013) on a 400 ML ice. Our calculation and measurement are somewhat rough, but we feel that they show a consistency with earlier work by others.

Table 1
Four Regions of the Infrared Spectra of Benzene Ices[a]

Region (cm^{-1})	Fundamentals	Approximate Description
3100–3000	ν_2, ν_7, ν_{13}, ν_{20}	CH stretches
1485–1465	ν_{19}	HCC bend and CC stretches
1045–1025	ν_{18}	HCCH wobble and CC stretches
710–650	ν_4, ν_{11}	Out-of-plane bending (ν_{11}), ring deformation (ν_4)

Note.
[a] For drawings of the fundamental vibrations of benzene, see Preuss & Bechstedt (2006) or page 118 of Herzberg (1945).

It is of interest to know if the small temperature-induced changes in Figure 3 were reversible with temperature. The answer was obtained by annealing the benzene sample. As there seems to be some confusion in the literature on what an annealing entails, we emphasize that it involves a warming followed by a cooling, such as a glassblower or potter might employ. Figure 4 again shows expansions of our four regions of interest for amorphous benzene. The spectra are of an ice made by vapor-phase condensation at 10 K, followed by *annealings* at 20, 30, 40, and 50 K, each spectrum being recorded at 10 K. It again is seen that the spectra hardly changed. As examples, peaks initially near 1477, 1035, and 677 cm^{-1} shifted by 0.5 cm^{-1} or less after the annealing cycles of Figure 4, the shifts were always to smaller values, and always irreversible. Note that a small degree of crystallization occurred during the ~10 minutes that a spectrum of amorphous benzene was measured at 50 K, as shown by the emergence of a weak shoulder near 1040 cm^{-1}, a very small peak near 708 cm^{-1}, and a slight broadening near 680 cm^{-1} in (e) in the bottom two panels of Figure 4. These three features did not appear in spectra of ices warmed to or annealed at 45 K.

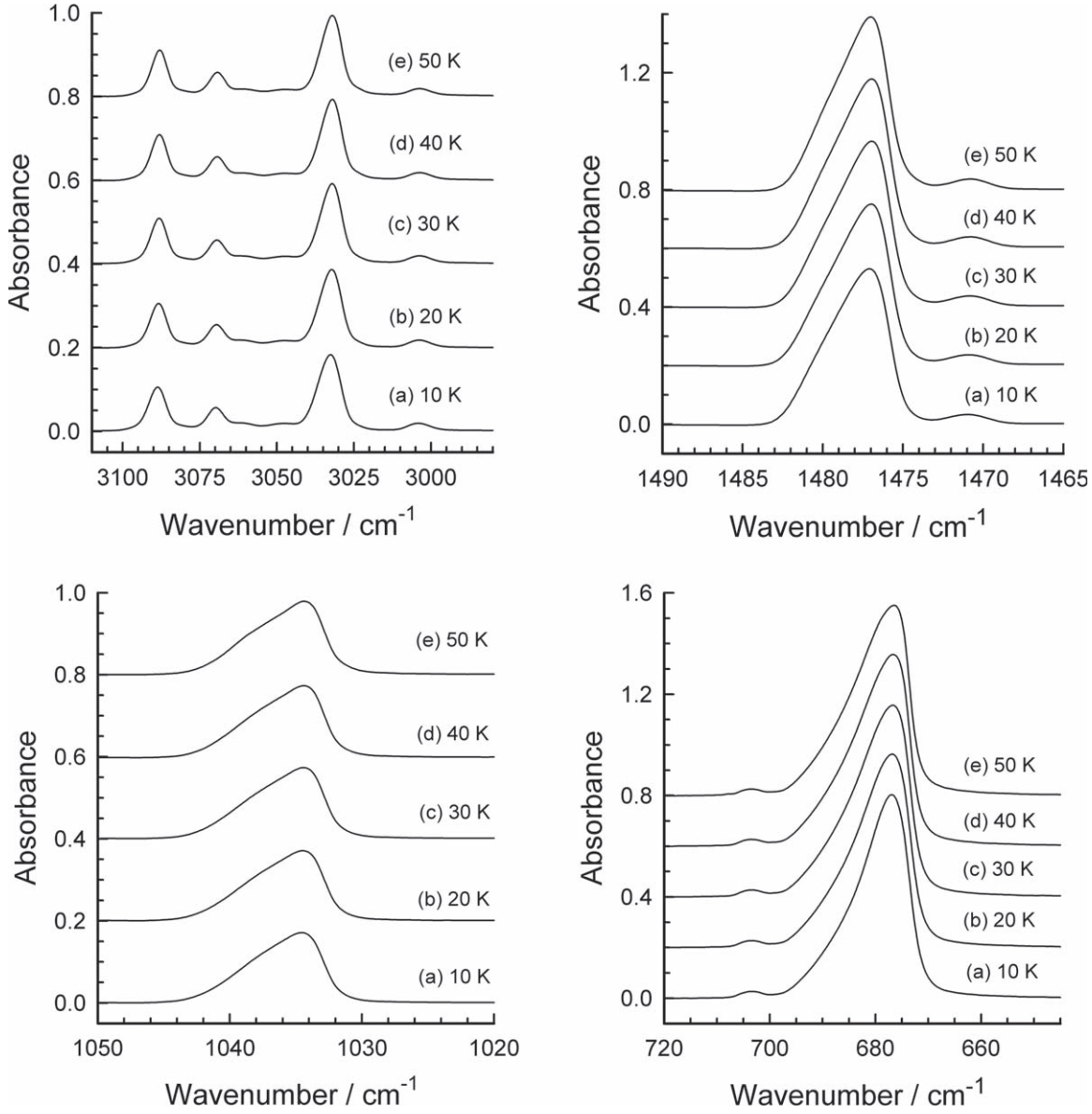

Figure 3. The IR spectrum (resolution = 1 cm^{-1}) of amorphous benzene (a) made by vapor-phase condensation at 10 K and warmed to (b) 20, (c) 30, (d) 40, and (e) 50 K. Spectra are offset vertically for clarity. The 10 K ice's thickness was about 1.9 μm, grown at ~3 μm hr^{-1}.

Besides making amorphous benzene ices at 10 K and then warming or annealing them, we also examined ices made by vapor-phase deposition at higher temperatures. Figure 5 summarizes the more important results. Spectrum (a) is for an amorphous benzene ice made at 10 K and then warmed to 45 K. Spectrum (b), showing several sharp peaks, is for a benzene ice made by deposition at 45 K with no additional temperature changes. Although (a) and (b) were recorded at the same temperature, and for ices grown at the same rate, differences are obvious. Comparing (b) to benzene ice spectra in our earlier paper (Hudson & Yarnall 2022), spectra from older papers (e.g., Anderson & Person 1962), or the spectra in the next section shows that the ice sample of (b) was partially crystalline. We attribute the crystallization at 45 K in (b), but not (a), to the energy released on condensation of room-temperature benzene vapor being sufficient to raise the ice's temperature above 45 K and promote crystallization. To test this idea, we lowered the deposition temperature to 40 K and grew a third ice at the same rate as in (b). The spectrum obtained is (c), in which the sharp peaks of crystalline benzene are still present but much less pronounced. Lowering the vapor's condensation rate for another 40 K deposition gave trace (d), which is essentially identical to what was expected for amorphous benzene (i.e., spectrum (d) of Figure 3). Other wavenumber regions for these four ices showed the same patterns seen in Figure 5, demonstrating clearly the influences of thermal history ((a) versus (b)), deposition temperature ((b) versus (c)), and deposition rate ((c) versus (d)) on the spectra of our vapor-deposited ices. We estimated the crystalline-to-amorphous ratio in the ices that gave (b) and (c) by comparing each spectrum to IR spectra of benzene ices that were essentially 100% amorphous and 100% crystalline. The result was that the crystalline-to-amorphous ratio is about 1:4 at 40 K and 1:2 at 45 K for spectra (c) and (b), respectively.

Our observation of a dependence of an ice's IR spectrum and crystallinity on deposition rate is not new; see, for example, our studies of amorphous C_2H_2, C_2H_4, and CH_4 (Hudson et al. 2014a, 2014b; Gerakines & Hudson 2015a), or our work on the

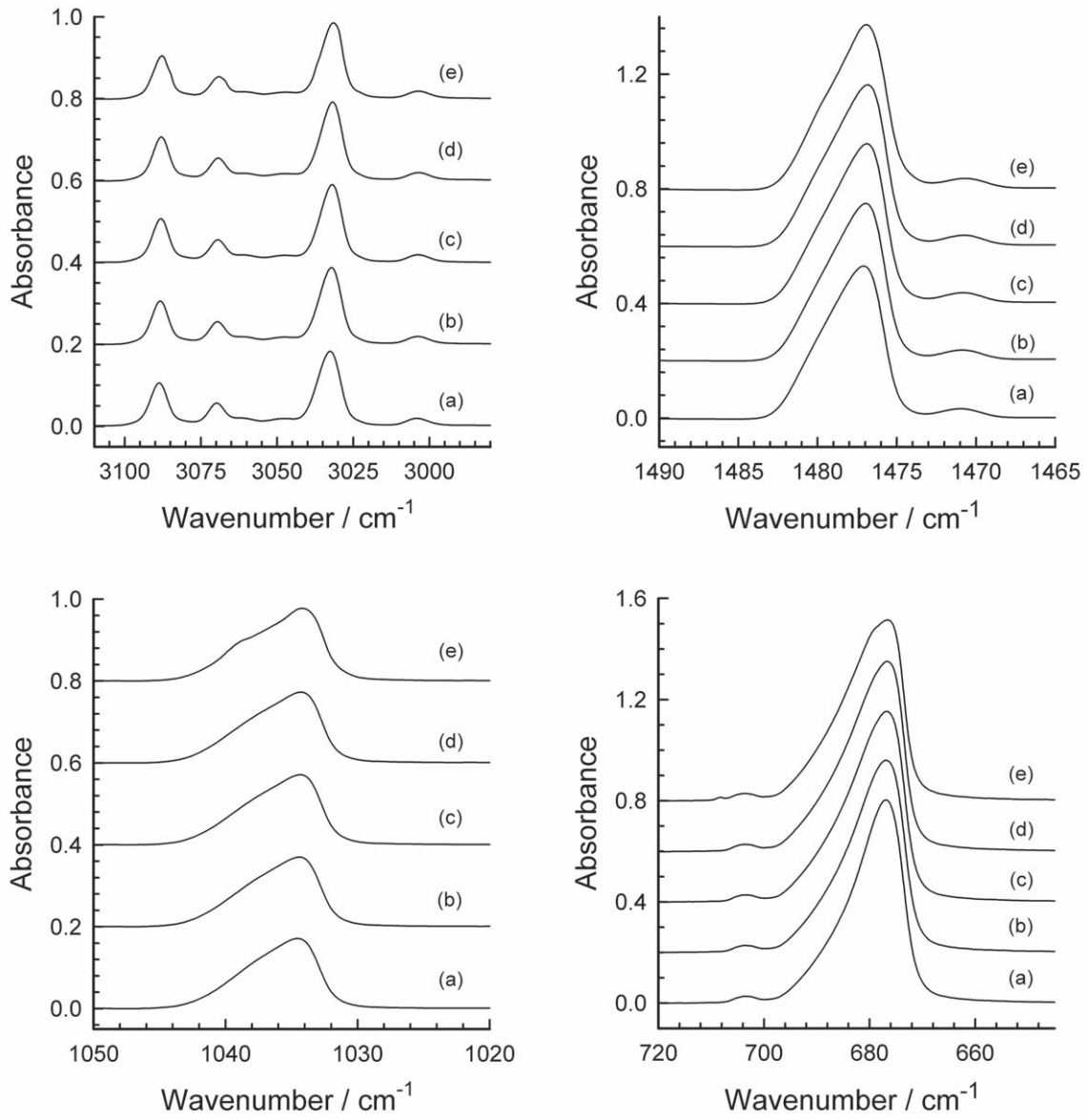

Figure 4. The IR spectrum (resolution = 1 cm^{-1}) of amorphous benzene (a) made by vapor-phase condensation at 10 K and after annealing at (b) 20, (c) 30, (d) 40, and (e) 50 K. Spectra are offset vertically for clarity, and each was recorded at 10 K. The 10 K ice's thickness was about 1.9 μm, grown at ~3 μm hr^{-1}.

isoelectronic molecules CO_2 and N_2O in Gerakines & Hudson (2015b) and Hudson et al. (2017), respectively. In each case, vapor-phase condensation resulted in the warming and, in some cases, the crystallization of an ice sample. Here again we were anticipated by earlier investigators. Mizuno et al. (2016) noted the challenge of making amorphous CO_2 due to the energy release from condensation, Takeda et al. (1990) made a similar observation about the preparation of amorphous ethane (C_2H_6), and Jacox (1962) did the same for the preparation of amorphous ethylene (C_2H_4). Both Beaumont et al. (1961) and Pryde & Jones (1952), in studies of amorphous H_2O-ice, mentioned the influence of deposition rate on the resulting ice. We emphasize that a high rate for vapor deposition onto a cold substrate can lead to experimental artifacts and a situation in which the IR spectra and the form of the resulting ice are altered. Conversely, we have encountered cases where a high deposition rate can be used to prepare crystalline ice phases that are thermodynamically, but not kinetically, favored (e.g., Hudson 2016, 2020).

3.3. *Crystalline C_6H_6 Ices at* T $\geqslant$ ~50 K

The temperatures of most interest in this work were those under about 50 K, for possible application to chemistry of TNOs and beyond, and above about 100 K, mainly for applications to Titan atmospheric-ice chemistry. Amorphous benzene ice was the solid of interest in the former, with crystalline benzene our focus in the latter. We made relatively few measurements between 50 and 100 K, and so we now turn from the lower temperatures to the higher ones.

Spectrum (b) of Figure 5 shows that a faster and more direct way to make crystalline benzene than warming an amorphous sample is simply to condense benzene vapor at a suitably high temperature in a vacuum system, but not so high that sublimation occurs, a point made long ago by Hollenberg & Dows (1962). In our previous paper on IR spectra of solid benzene, we used 100 K as our condensation temperature to make the crystalline solid. However, it has been argued that a deposition temperature of 120–130 K is needed for complete

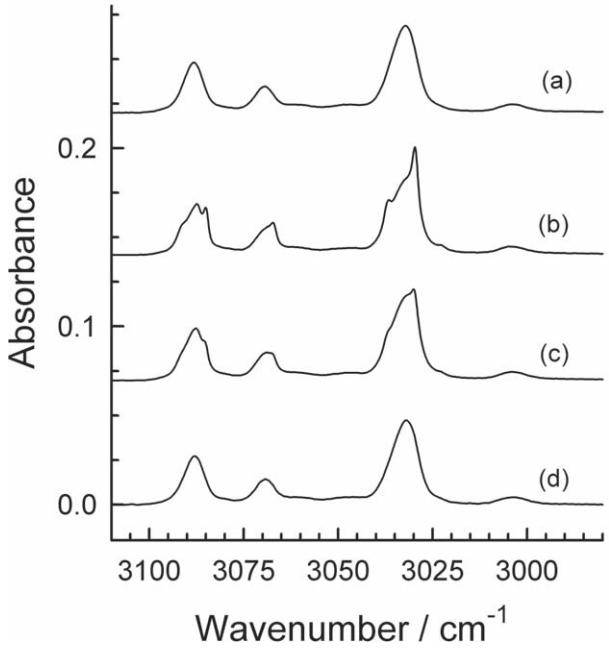

Thermal History	Ice T (K)	Deposition Rate (μm hr^{-1})
Warmed from 10 K	45 K	2
Ice made at 45 K	45 K	2
Ice made at 40 K	40 K	2
Ice made at 40 K	40 K	0.4

Figure 5. (a) Benzene deposited at 10 K and warmed to 45 K. (b) Benzene deposited at 45 K at ~2 μm hr^{-1}. (c) Benzene deposited at 40 K at ~2 μm hr^{-1}. (d) Benzene deposited at 40 K at ~0.4 μm hr^{-1}. Each ice had a thickness of ~0.5 μm and each spectrum had a resolution of 1 cm^{-1}. Spectra are offset vertically for clarity.

crystallization (Nna-Mvondo & Anderson 2022). We address this concern with four IR regions in Figures 6 and 7. Each row of each figure has spectra for two different ices recorded at the same temperatures. In each row, Ice #1 was made by condensation at 100 K and warming to 130 K, while Ice #2 was made by condensation at 130 K followed by cooling to 100 K, with all spectra recorded at the 4 cm^{-1} resolution of Nna-Mvondo & Anderson (2022). It is seen that at this resolution essentially the same IR spectrum results regardless of whether one goes from 100 to 130 K (Ice #1) or from 130 to 100 K (Ice #2). Put more plainly, attempts to use spectra at this resolution to find significant structural differences in benzene ices would seem an exercise in overinterpretation.

The spectral resolution in Figures 6 and 7 is quite low compared to both past (e.g., Anderson & Person 1962) and current (Hudson & Yarnall 2022) studies, so in Figures 8 and 9 we present results for the same two ices at the same temperatures, but at a higher resolution, 0.5 cm^{-1}. Small differences can be found with effort, but the overwhelming impression is the same as before, that the four IR spectra in each row are nearly the same, suggesting comparable crystallinity for the two ices. However, we hasten to mention a few differences that could have an important application. The lower row of Figure 9 shows that the IR spectrum of crystalline benzene has a small, sharp, distinct feature near 707 cm^{-1} at 100 K. On warming to 130 K, the peak's position decreased by ~0.7 cm^{-1}. The shift also is easily seen in Figure 3 of Mouzay et al. (2021). In our Figure 10 we plot the peak's position over a range of temperatures, since such data could, in principle, be used to estimate temperatures of Titan's benzene ices. Figure 10 also shows positions of the two other components of the strong ν_{11} band of crystalline benzene near 680 cm^{-1} as a function of temperature. The figure shows that the difference in spacing of the two peaks changes with temperature. Table 2 gives the positions of all three of the IR features of Figure 10. (Note that the ν_{11a} peak near 708 cm^{-1} is not the crystalline-ice counterpart of the broad, weak ν_4 feature of amorphous benzene near 703 cm^{-1}. The latter is lost on crystallization.) Changes in position with temperature for peaks in other IR regions were small and complicated by overlapping bands. In all cases, shifts in peak positions in our crystalline ices were reversible with heating and cooling, the opposite of the case for amorphous benzene ices. A few measurements of the integrated intensities (i.e., band areas) of these same IR features were made at 60–140 K. We found, in agreement with Hollenberg & Dows (1962), that the variation was on the order of 1% or less; see Hudson & Yarnall (2022) for band strengths and optical constants of crystalline benzene at 100 K.

Having investigated the role of condensation rate on the IR spectra of amorphous benzene ices (Figure 5), we then did the same with crystalline benzene ices. We grew ices at 100 K at rates that gave an increase in thickness of about 0.55–74 μm hr^{-1} for an ice thickness of about 0.83 μm in each case; see Figure 11 for spectra of four such ices. Comparing these spectra shows that the profile of the strong feature of crystalline benzene near 680 cm^{-1} varied with deposition rate. (Few differences were seen in other IR regions, and a rate of only 0.55 μm hr^{-1} gave nothing not seen at 2.5 μm hr^{-1}.) None of the IR-forbidden peaks of amorphous benzene were present in any of these spectra, demonstrating crystallinity for all four ices. The position and height of the small ν_{11a} peak on the left in each spectrum shows that the four ices had the same thickness and temperature. In short, all four spectra are for crystalline benzene at 100 K, but their thermal histories differ, the spectra suggesting structural differences in the samples. For an earlier study of how deposition rate can alter a crystalline ice's IR spectrum, see the CS_2 work of Yamada & Person (1964).

Figure 11 shows that the shape of crystalline benzene's 680 cm^{-1} band is indeed variable. Another comparison of results is given in Figure 12 for four ices at 130 K, with data from three laboratories. In (a) we show the same spectrum as in

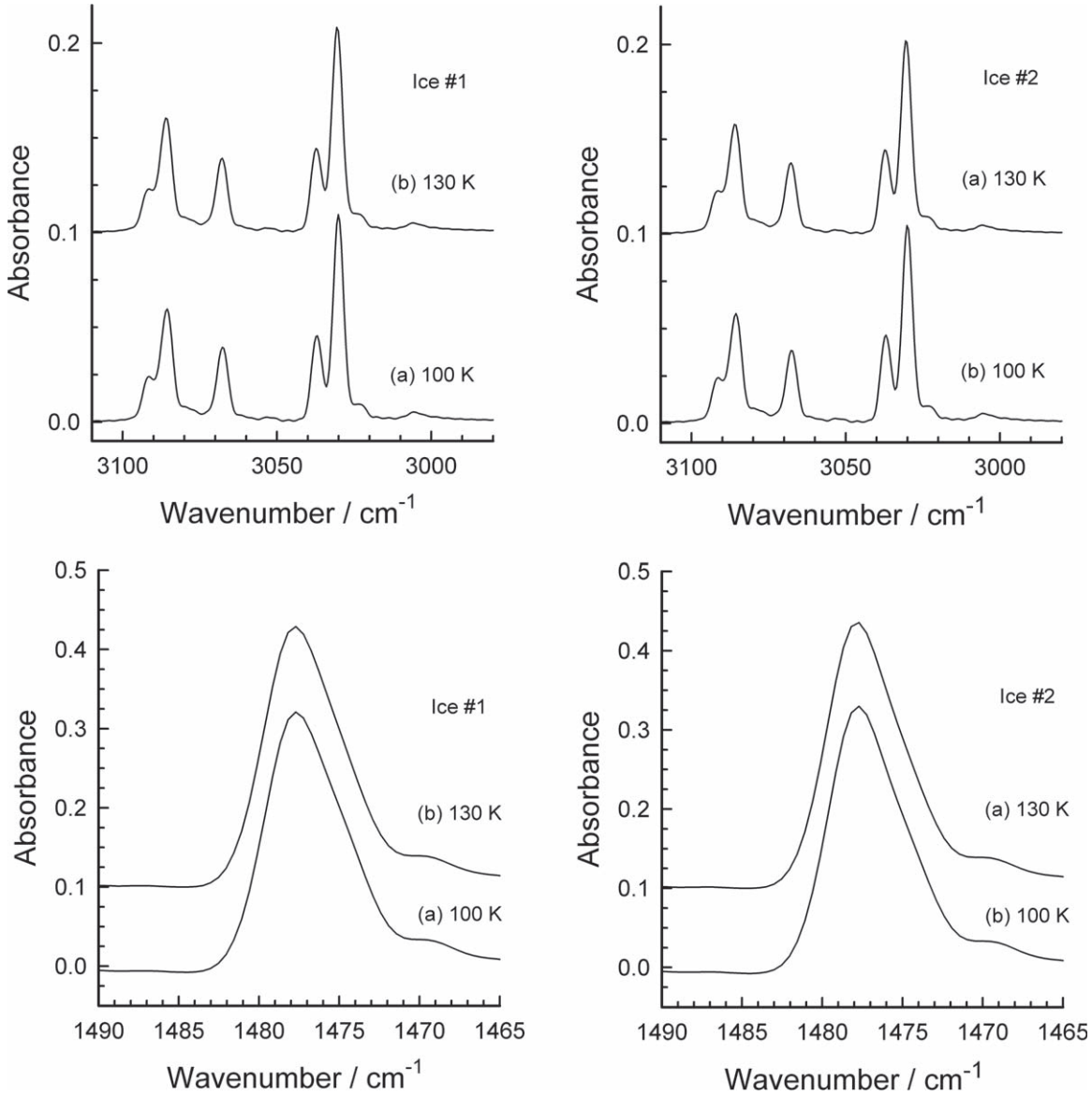

Figure 6. Two regions of the IR spectrum of crystalline benzene. Ice #1 (left) was grown at 100 K and warmed to 130 K. Ice #2 (right) was grown at 130 K and cooled to 100 K. Each ice had a thickness of ∼0.83 μm and was grown at ∼1.3 μm hr^{-1}. The spectral resolution was 4 cm^{-1}. Spectra are offset vertically for clarity.

(a) of Figure 11, which we recorded at a sufficiently low deposition rate that the ice and the IR band shape were little, if at all, altered by condensation energy. Spectrum (b) is for an ice we made at 10 K and then warmed to 130 K. Near 680 cm^{-1}, a peak and a weak shoulder can be seen near the positions of the two highest peaks of (a). Spectra (a) and (b) were recorded with 0.5 cm^{-1} resolution. Spectrum (c) was recorded in a reflection mode for an ice made at 16 K and then warmed to 130 K (Mouzay et al. 2021), with 1 cm^{-1} resolution. A peak near 678 cm^{-1} can be seen, along with a very faint shoulder near 681 cm^{-1}. Spectrum (d) was calculated (ice thickness = 1 μm, $n = 1.62$) using the optical constants determined by Nna-Mvondo & Anderson (2022) from IR spectra with a resolution of 4 cm^{-1}, the ice being grown at 130 K.

Variations among (a) to (d) in Figure 12 are clear, but all four spectra are for crystalline benzene at the same temperature. Differences between (a) and (b) are due simply to different thermal histories, and are not particularly surprising. Trace (c) varies from (a) because of differences in thermal history, spectral resolution, and the reflection mode used for the measurement. The resolution of the IR spectra used to calculate (d) is sufficiently low (4 cm^{-1}) that it is hard to determine if two peaks are present near 680 cm^{-1}, much less to determine their positions. We conclude from Figure 12 that care is needed in lab-to-lab comparisons of crystalline C_6H_6 IR spectra in the 680 cm^{-1} region.

3.4. Crystallization of C_6H_6 Ices

We examined the isothermal crystallization of amorphous benzene ices grown at 10 K to a thickness of about 0.5 μm at ∼3 μm hr^{-1} and then warmed to 45, 50, or 55 K. We followed each ice's conversion using the growth of the sharp crystalline-ice peak near 708 cm^{-1} and the fall in the IR-forbidden peak near 1177 cm^{-1} for amorphous benzene. The ice sample held at 45 K reached about 50% crystallization in about 24 hr. The ice held at 55 K required only about 5 minutes for 50% crystallization. Between these was the ice held at 50 K, for which results are shown in Figure 13, where it is seen that about 90

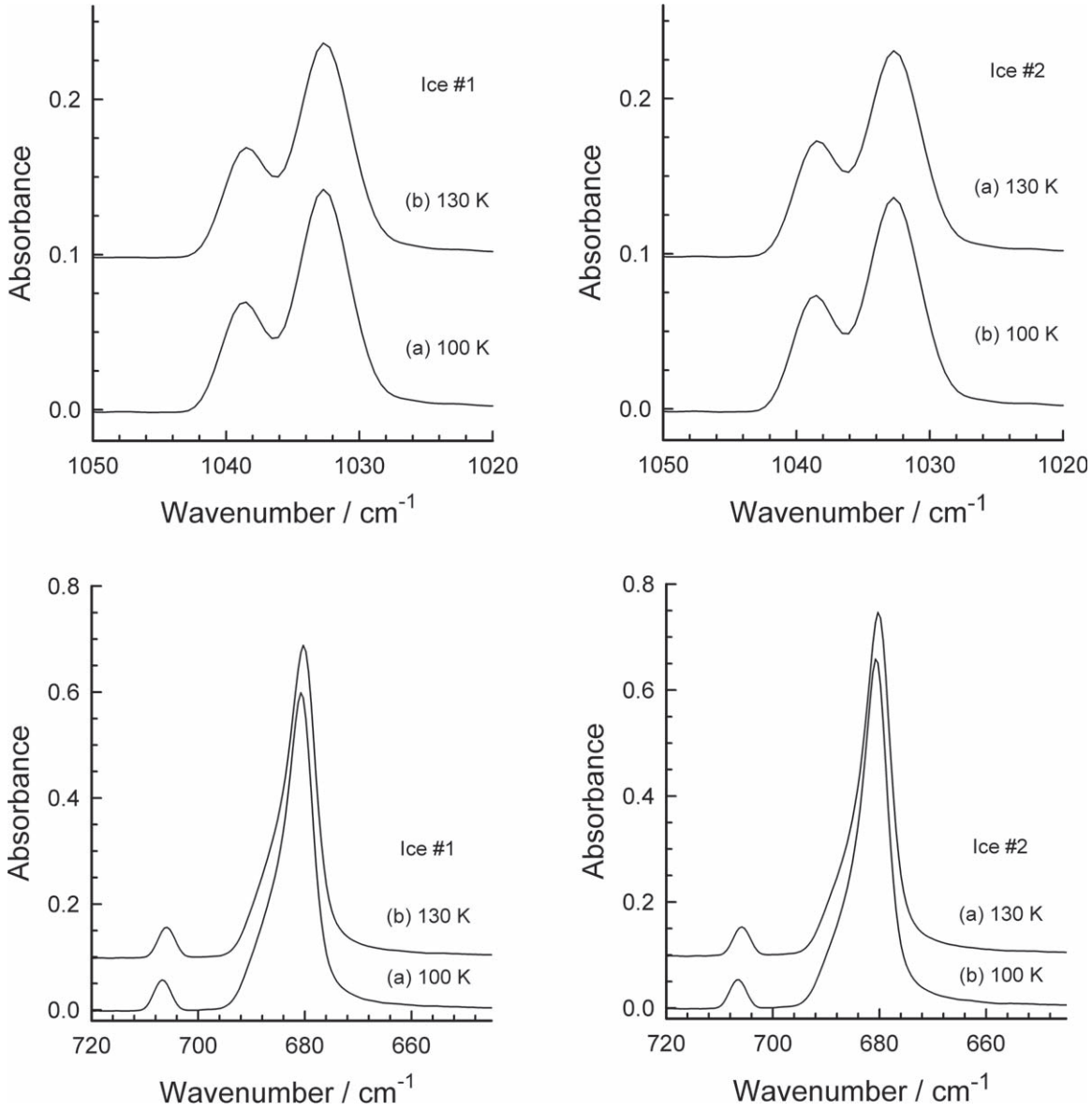

Figure 7. Two regions of the IR spectrum of crystalline benzene. Ice #1 (left) was grown at 100 K and warmed to 130 K. Ice #2 (right) was grown at 130 K and cooled to 100 K. Each ice had a thickness of ∼0.83 μm and was grown at ∼1.3 μm hr^{-1}. The spectral resolution was 4 cm^{-1}. Spectra are offset vertically for clarity.

minutes were needed for the sample to rise to 50% crystallization. The three ices studied showed that the rate of crystallization of amorphous benzene depends on the ice's temperature.

The curves in Figure 13 possess the induction period and sigmoidal shape expected for a solid–solid phase transition (Rao & Rao 1978; Wang et al. 2005). It should be possible to repeat the measurements just described, and with more temperatures, to probe the kinetics of amorphous benzene's crystallization. The curve for the fall of absorbance in Figure 13 corresponds to the decreasing amount of amorphous ice in the sample, and is based on the IR-forbidden feature at 1177 cm^{-1}. As this is an inherently weak band, thicker benzene samples would help to reduce the uncertainties in the measurement. For examples of such work, see the studies of Jenniskens & Blake (1996), Dohnálek et al. (2000), and Mitchell et al. (2017).

Accompanying our benzene ices' crystallization was the loss from the original spectra of all IR features due to amorphous C_6H_6, such as the three in Figure 2. Also, as the amorphous benzene ice crystallized, the spectra showed numerous isosbestic points, such as those near 1480, 1477, 1475, 1472, 1470, 691, and 679 cm^{-1} in Figure 14. These isosbestic points can serve as reference data for lab-to-lab comparisons. They also suggest that no other processes were occurring during the ice's crystallization. For two examples of isosbestic points from the lab-astrophysics community, see Figure 4 of Tsuge et al. (2020) for the crystallization of amorphous CO_2.

4. Discussion

4.1. Making and Comparing Benzene Ices

Our spectra of amorphous benzene in Figure 3 agree with those of Mouzay et al. (2021) in terms of band shapes and positions and in showing only small changes on warming amorphous benzene from 16 to 50 K. However, as the spectra of Mouzay et al. (2021) were obtained in a reflection mode, it is not surprising that the relative intensities of their IR bands do not match ours. For example, in our spectra the ratio of the

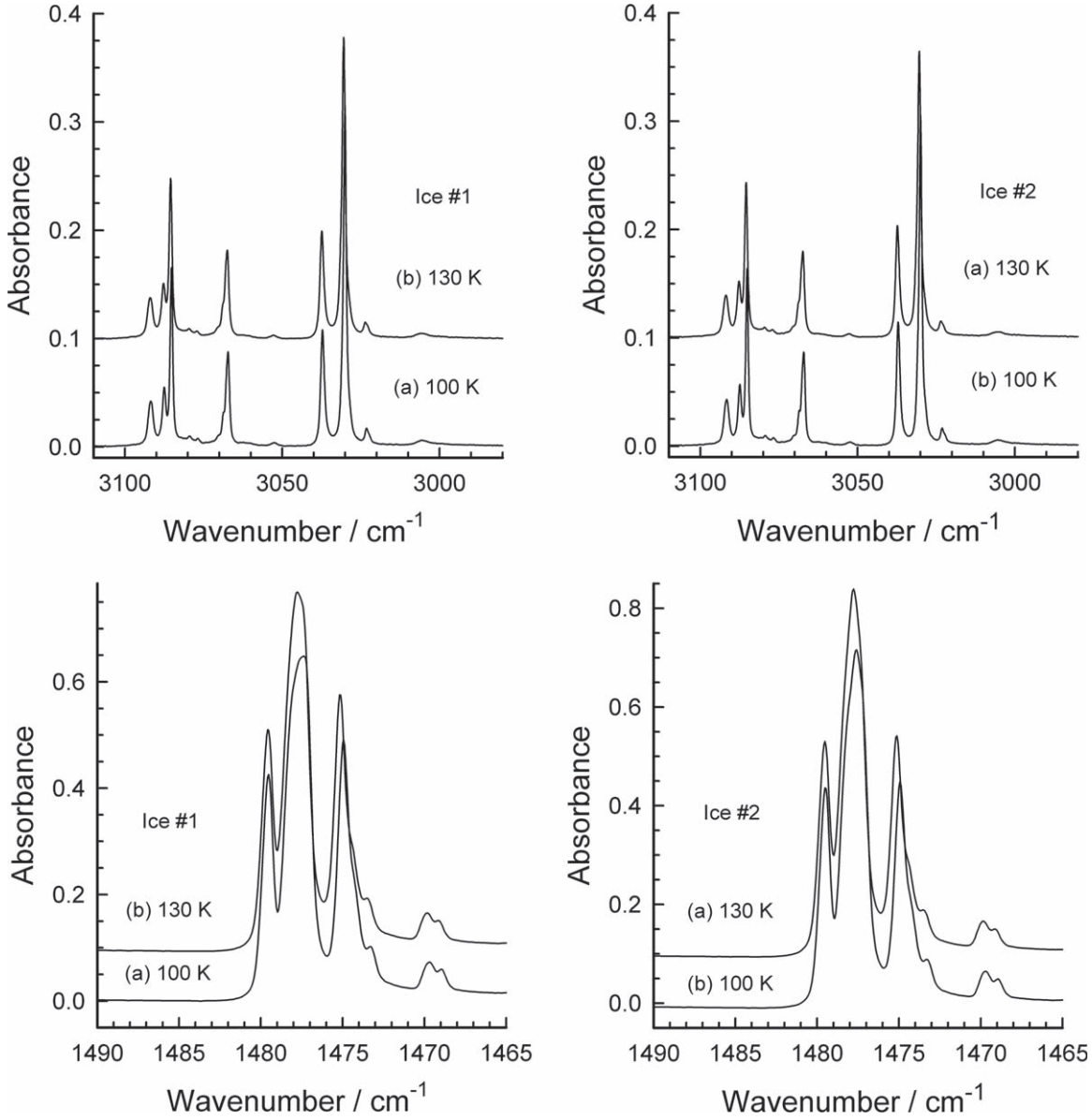

Figure 8. Two regions of the IR spectrum of crystalline benzene. Ice #1 (left) was grown at 100 K and warmed to 130 K. Ice #2 (right) was grown at 130 K and cooled to 100 K. Each ice had a thickness of ∼0.83 μm and was grown at ∼1.3 μm hr^{-1}. The spectral resolution was 0.5 cm^{-1}. Spectra are offset vertically for clarity.

absorbance of the IR peak near 680 cm^{-1} to that of the peak near 1035 cm^{-1} is about 4:1, but in the spectra of Mouzay et al. (2021) the ratio is only about 2:1, as seen in our Figure 15. Comments similar to these for amorphous benzene also apply to comparisons involving the spectra of crystalline benzene.

The benzene-ice IR spectra of Nna-Mvondo & Anderson (2022) were recorded, like ours, in transmission, and are in reasonable agreement with our work in terms of peak positions and relative intensities. However, in a separate paper it was shown that while the IR spectra of our crystalline benzene ices at 0.5 cm^{-1} resolution are in excellent agreement with literature spectra, those of Nna-Mvondo & Anderson, at a much lower resolution, are not (Hudson 2022). The benzene spectra shown by Nna-Mvondo & Anderson (2022) were for a single IR resolution and benzene condensation rate, with all ices having about the same thickness. Also, that paper's spectra were for ices condensed at specific temperatures and with the spectra shown being recorded only at those same temperatures. This results in a convolution of (i) spectral features due to an ice's formation temperature, and (ii) spectral features due to the temperature at which an ice's spectrum was recorded, making it difficult to independently evaluate each variable's influence. Our Figures 6–9 permit such an independent evaluation at two spectral resolutions and two temperatures, the result being that we find relatively few differences between IR spectra of crystalline benzene for ices made at 100 K and warmed to 130 K or vice versa.

A third literature comparison should be mentioned here. The benzene-ice paper of Szczepaniak & Person (1972) appears to have received little or no attention over the past half-century by laboratory investigators of planetary and interstellar ices, including the present authors. However, that same paper includes a transmission-IR spectrum of amorphous benzene and one of crystalline benzene, both at 1 cm^{-1} resolution with ice thicknesses measured by interferometry using explicitly stated values of ice density and refractive index, as well as specified ice temperatures and deposition rate. The authors' spectra are on a small scale with several overlapping traces, but

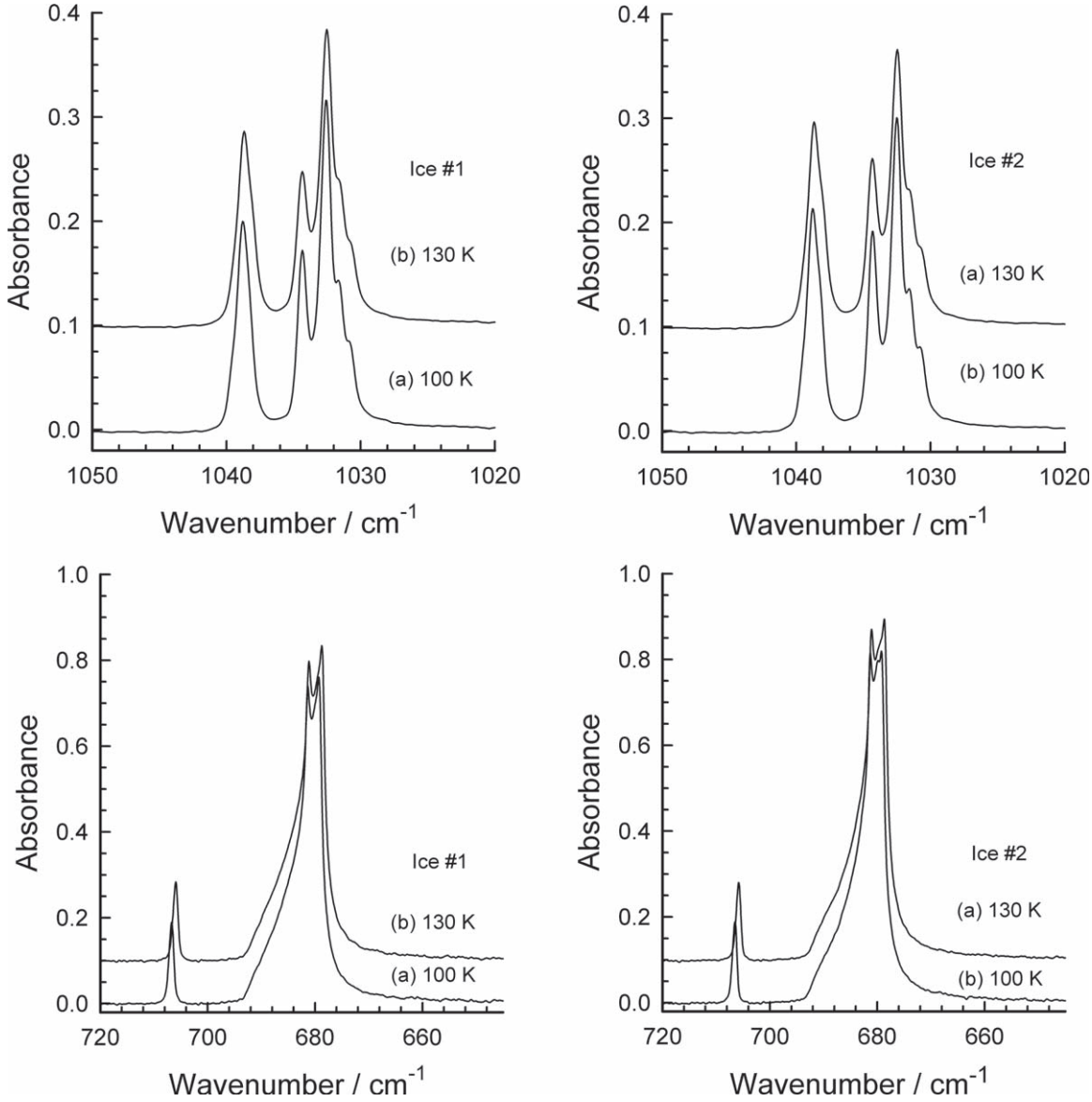

Figure 9. Two regions of the IR spectrum of crystalline benzene. Ice #1 (left) was grown at 100 K and warmed to 130 K. Ice #2 (right) was grown at 130 K and cooled to 100 K. Each ice had a thickness of ∼0.83 μm and was grown at ∼1.3 μm hr^{-1}. The spectral resolution was 0.5 cm^{-1}. Spectra are offset vertically for clarity.

they clearly show the IR features that we have presented in this paper, including IR-forbidden bands in amorphous, but not crystalline, benzene. The band strengths tabulated by Szczepaniak & Person (1972) are missing a factor of 10^6, but once that is included then the authors' relative and absolute IR intensities are in good agreement with ours (Hudson & Yarnall 2022).

That our ices that were vapor deposited at 100 K and above were essentially 100% crystalline is based on multiple observations. First, our IR spectra agree with those in the literature already cited. Second, there is no evidence from calorimetric studies (Oliver et al. 1948) for solid–solid phase transitions for crystalline benzene under vacuum conditions, and we did not observe anything that could be interpreted as a phase change until sublimation. Third, only temperature-reversible changes were seen in our 100 K spectra, in contrast to the irreversible changes for amorphous benzene. Fourth, we measured the densities of benzene ices made at 100 and 130 K and found that the values were close to those from diffraction studies of crystalline benzene and also that the densities decrease slightly with increasing temperature, as reported by Fortes & Capelli (2018). Finally, none of the IR-forbidden features of amorphous benzene were seen in the spectra of our ices made at 100 K and above. This last point is a particularly powerful indicator of crystallinity, one based on IR selection rules for a specific solid structure derived from diffraction measurements. Put another way, IR-forbidden transitions in an ice's spectrum imply that the sample is at least partially amorphous; their absence implies crystallinity.

In contrast to the above, it has been suggested that a lack of ice sublimation at a specific temperature is one criterion for an ice's crystallinity (Nna-Mvondo & Anderson 2022). Since sublimation can be observed over a range of temperatures depending on an ice's vapor pressure, a vacuum chamber's pressure, and the length of time over which a measurement is made, we do not recommend a lack of sublimation as an indication of crystallinity. We recently have explored benzene sublimation in a separate investigation (Hudson et al. 2022a).

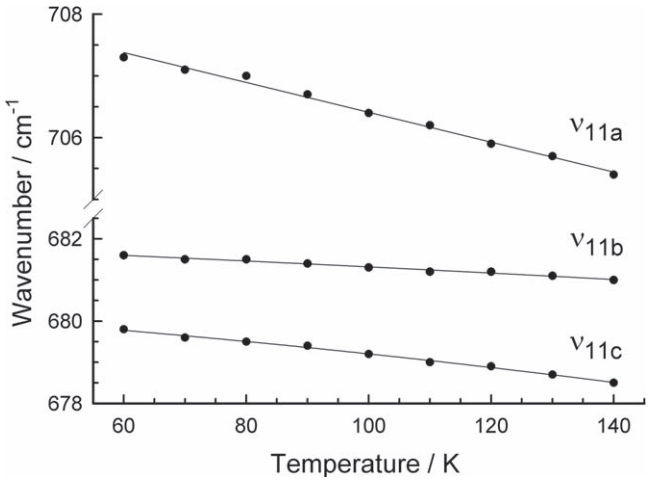

Figure 10. Positions of three IR peaks of crystalline benzene as a function of temperature. Changes in position were reversible with temperature. Spectra from eight ices were used to create the figure. The thickness of each ice was ~1 μm and the spectral resolution was 0.5 cm^{-1}.

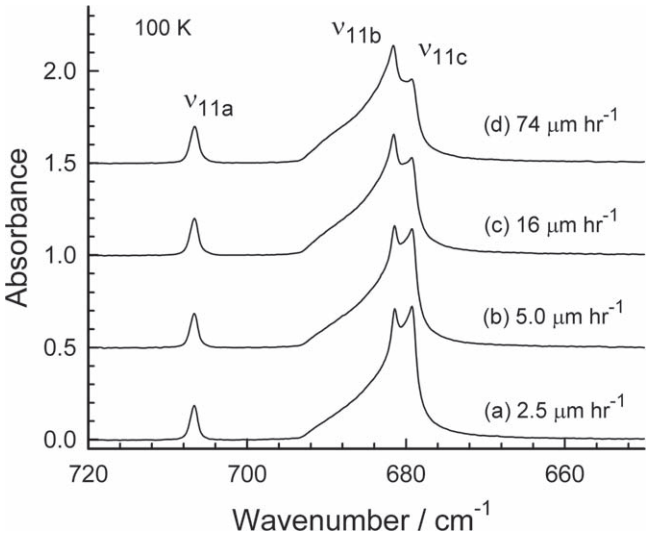

Figure 11. Spectra of crystalline benzene made at 100 K by vapor-phase deposition at four different deposition rates. The thickness of each ice was about 0.83 μm and the spectral resolution was 0.5 cm^{-1}. Spectra were recorded at 100 K and are offset vertically for clarity.

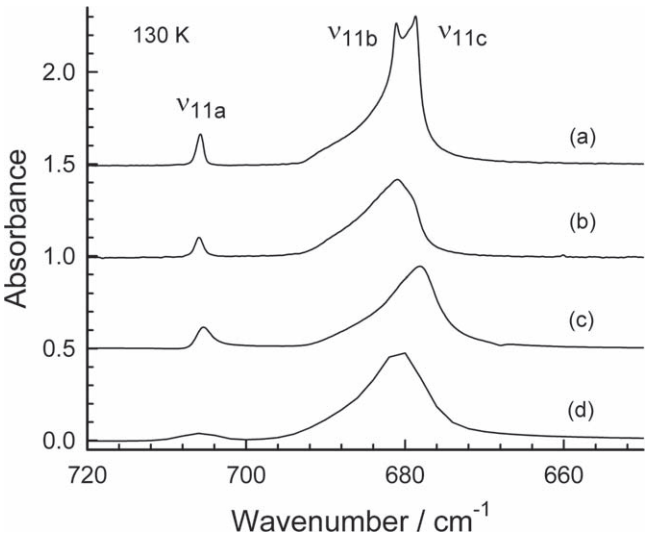

Figure 12. Four IR spectra of crystalline benzene at 130 K. (a) This work, ice made at 130 K. (b) This work, ice grown at 10 K and warmed to 130 K. (c) Ice of Mouzay et al. (2021), grown at 16 K and warmed to 130 K. (d) Ice of Nna-Mvondo & Anderson (2022), grown at 130 K. Resolutions are 0.5 cm^{-1} for (a) and (b), 1 cm^{-1} for (c), and 4 cm^{-1} for (d). Spectra are offset vertically for clarity. Spectrum (c) was recorded in a reflection mode, but the others are conventional transmission spectra.

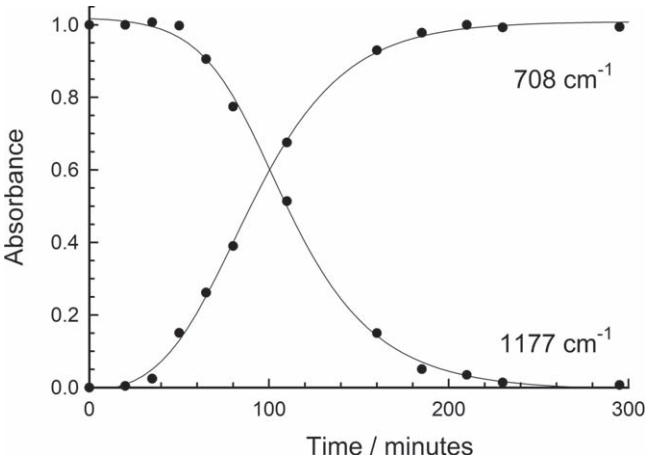

Figure 13. Crystallization of amorphous benzene at 50 K as followed by the growth of the crystalline-benzene peak near 708 cm^{-1} and the fall of the amorphous-benzene peak near 1177 cm^{-1}. The absorbance for the crystalline-ice peak has been scaled (normalized) to its final value, while the absorbance for the amorphous-ice peak has been scaled to its initial value.

The influence we found of thermal history on the IR spectrum of a benzene ice made by vapor-phase deposition is as expected. As already seen, traces (a) and (b) of our Figure 5 show that the spectrum of a benzene ice warmed from 10 to 45 K can be dramatically different from that of an ice grown at 45 K. Some years ago, we presented a similar difference for H_2O-ices, showing that amorphous H_2O-ice made at 14 K could be crystallized by warming to over 140 K, but crystalline H_2O-ice also could be made by condensation of H_2O vapor at temperatures as low as 120 K (Moore et al. 2001). Ishii et al. (1996) presented similar observations for solid benzene, with an amorphous ice showing Raman spectral features for crystallinity after warming from 17 to 58 K, but the same Raman bands also appearing in an ice made by a 45 K deposition. This behavior for both solid H_2O and solid C_6H_6 can be attributed, as already mentioned, to the energy released on condensation of the room-temperature vapor used to make ices. We suggest that many of the IR spectra of solid benzene between 30 and 60 K in Nna-Mvondo & Anderson (2022) are mixtures of amorphous and crystalline ice that have been "self-annealed" by the high deposition rate used, as in (b) and (c) of our Figure 5. Put differently, the ices' compositions and IR band shapes are artifacts of rapid condensation. Slower rates will yield different amorphous/crystalline ratios in the ices as well as IR band shapes closer to those shown here and from Mouzay et al. (2021).

4.2. Extraterrestrial Benzene Ices

There are two immediate astrochemical implications from the meager IR changes seen on either warming or annealing amorphous benzene ices. First, there are no mid-IR features that can be used to easily and remotely determine the

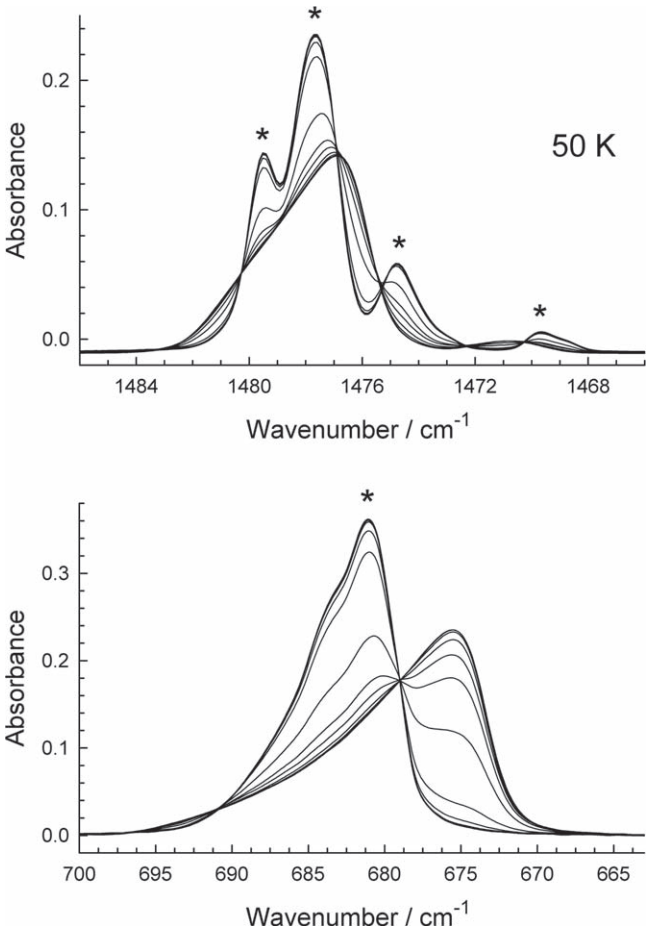

Figure 14. Crystallization of amorphous benzene at 50 K showing isosbestic points in two IR regions. The amorphous ice was grown at ~3 μm hr^{-1} at 10 K to a thickness of about 0.5 μm and then warmed to 50 K. The peaks near 1477 and 675 cm^{-1} are decreasing during crystallization, while the ones marked by asterisks (*) are increasing (rising).

temperature of amorphous benzene on an extraterrestrial body, such as a TNO. We found that the positions of the IR peaks changed irreversibly with temperature by less than 1 cm^{-1}, and in most cases just a few tenths of a cm^{-1}. (In other words, warming can shift a peak's position slightly, but recooling does not return the position to its original value.) Second, the small spectral changes seen for amorphous benzene with temperature mean that the band strengths, absorption coefficients, and optical constants we have published for amorphous benzene at 10 K ice (Hudson & Yarnall 2022) can be used for up to ~50 K. This should cover the temperatures expected for interstellar, cometary, and TNO ices. This temperature range, coupled with the influence of ionizing radiation, almost guarantees that crystalline benzene will not be found in such environments.

The situation regarding crystalline benzene is quite different from that with amorphous benzene. Of all the IR features of benzene ices in our figures, the band near 680 cm^{-1} (ν_{11}) probably has the highest combination of IR strength and relevance to astronomical observations, given its detection in Titan's atmosphere. Therefore, it is important to emphasize that this band possesses a variability not seen with other IR absorbances of solid benzene. Figure 11 shows that crystalline-benzene ices of the same thickness, but grown at different rates, can show differences in the relative heights of the two

Table 2
Positions (cm^{-1}) of Three Infrared Peaks of Crystalline Benzene[a]

T/K	ν_{11a}	ν_{11b}	ν_{11c}
140	705.4	681.0	678.5
130	705.7	681.1	678.7
120	705.9	681.2	678.9
110	706.2	681.2	679.0
100	706.4	681.3	679.2
90	706.7	681.4	679.4
80	707.0	681.5	679.5
70	707.1	681.5	679.6
60	707.3	681.6	679.8

Note.
[a] Positions are averages of up to four measurements. Uncertainties in the form of standard deviations are less than ±0.05.

components of the ν_{11} feature. In a previous paper, we showed that similar variations are seen with ices of different thickness, but grown at the same rate (Hudson & Yarnall 2022). In agreement with Mouzay et al. (2021), we also have observed that only a single, less-resolved IR feature is present near 680 cm^{-1} when crystalline-benzene ices are made by warming amorphous benzene (i.e., (b) of Figure 12). Clearly, the conditions of ice growth and thermal history influence the shape of the 680 cm^{-1} band and the relative heights of its two components. Therefore, we suggest caution in using either the shape of the ν_{11} band or the relative heights of its two components in interpreting either laboratory or observational results.

As for the underlying causes of the variations just mentioned, we simply note that the conditions of an ice's growth can influence the resulting crystals' sizes, shapes, and orientations, which in turn can alter IR spectra. One is reminded, for example, of how increases in crystal size can produce scattering, reflection, and broader IR bands of compounds in potassium bromide pellets (e.g., Sato et al. 1969; Baraldi 1979) or how IR bands can change with particle shape (e.g., Imai et al. 2009). The highest condensation rate we used to grow crystalline benzene was far greater than the rates we usually adopt, even larger than the high rate (~34 μm hr^{-1}) of Nna-Mvondo & Anderson (2022). We suggest that such fast condensations not only anneal the samples but also influence the sizes, shapes, and orientations of the crystals themselves, giving rise to spectral differences that we have reported here, such as in Figure 11. We further suggest that the *distributions* of crystal sizes, shapes, and orientations in ices rapidly grown can differ from those in ices grown and annealed more slowly. With all of this in mind, it remains to be seen whether ices grown by very rapid condensation (i.e., Figure 11) of room-temperature (~300 K) benzene vapor are relevant, realistic analogs of Titan's atmospheric benzene ices.

4.3. Future Work

Before ending, we offer some areas for future investigation. Perhaps most needed is greater insight into the nature of benzene crystals both in the laboratory and in the atmosphere of Titan. Diffraction measurements along the lines of the H_2O-ice study of Jenniskens & Blake (1996) could deliver information on sizes of benzene crystals made under various conditions. Further study of the mixed amorphous+crystalline ices of Nna-Mvondo & Anderson (2022) might reveal if the

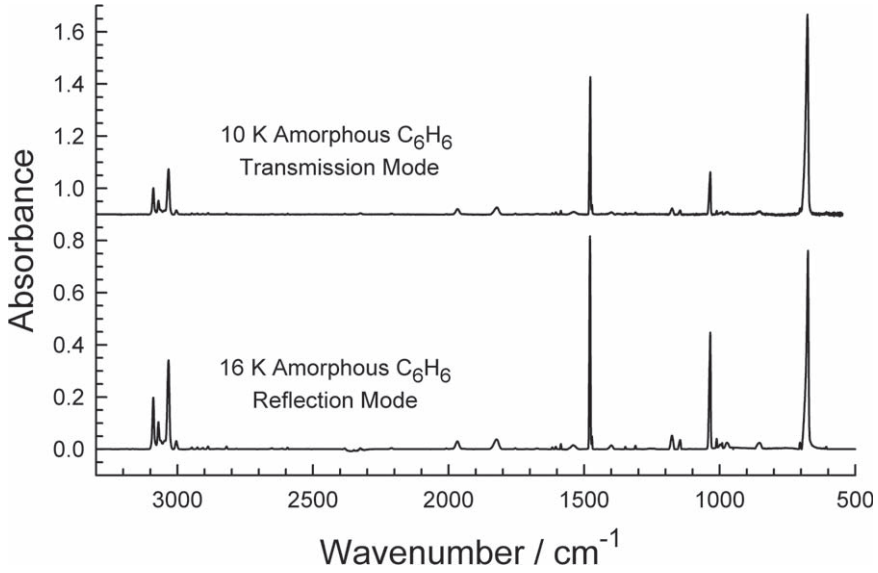

Figure 15. The spectrum of amorphous benzene recorded in a transmission mode (upper, this work) compared to the spectrum recorded in a reflection mode (lower, Mouzay et al. 2021). The upper spectrum is the same as in Figure 1, but scaled vertically to match the lower spectrum (ice thickness unknown) at 680 cm^{-1}, and is offset vertically for clarity.

amorphous-to-crystalline ratio depends on ice thickness, among other variables. It also would be interesting to know if the crystalline component grows throughout the sample or only at the ice's surface at the vacuum–ice interface. The rate of benzene crystallization, including its temperature dependence, has yet to be fully quantified, including the possible influence of the presence of a second compound. Much more work also is needed to better characterize the near-IR shapes, areas, positions, and intensities of amorphous and crystalline benzene over a range of temperatures.

5. Conclusions

This paper has presented new results from multiple laboratory measurements on solid benzene from 10 to 140 K. Given the many variables explored, it is appropriate to summarize the results obtained and the trends observed:

The small reflection-IR spectral changes reported for amorphous benzene on warming from 16 K have been confirmed by transmission-IR spectra, and annealing measurements have shown that all such changes are irreversible. Small temperature-dependent IR changes also have been found for crystalline benzene, but in contrast to those for amorphous ices such changes are reversible. Changes in position with temperature for one weak, but sharp, IR feature and two much stronger ones have been shown for the 700 cm^{-1} region.

The separate influences of temperature and condensation rate on the formation of benzene ices have been demonstrated for the first time, along with the possibility of artifacts arising from them. We have shown that high condensation rates can anneal both amorphous and crystalline benzene ices, altering their structure and IR spectra. The importance of comparing IR spectra of ices at the same temperature has been stressed.

We have documented the temperature dependence of amorphous benzene's crystallization, and have identified isosbestic points in the associated IR spectra.

We have shown how IR-forbidden transitions can be used to identify ices that are partially or wholly amorphous.

We suggest that differences in the IR spectra of crystalline ices at the same temperature do not necessarily imply partial crystallization, but rather that such differences can arise from the many variables involved in an ice's growth.

We acknowledge support from NASA's Planetary Science Division Internal Scientist Funding Program through the Fundamental Laboratory Research (FLaRe) work package at the NASA Goddard Space Flight Center. Yukiko Y. Yarnall is thanked for assistance with some of the measurements.

ORCID iDs

Reggie L. Hudson https://orcid.org/0000-0003-0519-9429
Perry A. Gerakines https://orcid.org/0000-0002-9667-5904

References

Anderson, G. R., & Person, W. B. 1962, JChPh, 36, 62
Baraldi, P. 1979, AnaCh, 51, 1597
Baratta, G. A., Leto, G., Spinella, F., Strazzulla, G., & Foti, G. 1991, A&A, 252, 421
Barth, E. 2017, P&SS, 137, 20
Beaumont, R. H., Chihara, H., & Morrison, J. A. 1961, JChPh, 34, 1456
Bertie, J. E., & Keefe, C. D. 2004, JMoSt, 695, 39
Bertie, J. E., Labbé, H. J., & Whalley, E. 1969, JChPh, 50, 4501
Bézard, B., Drossart, P., Encrenaz, T., & Feuchtgrube, H. 2001, Icar, 154, 492
Callahan, M. P., Gerakines, P. A., Martin, M. G., Peeters, Z., & Hudson, R. L. 2013, Icar, 226, 1201
Cernicharo, J., Heras, A. M., Tielens, A. G. G. M., et al. 2001, ApJL, 546, L123
Cherchneff, I. 2011, in EAS Publications Ser. 46, PAHs and the Universe: A Symposium to Celebrate the 25th Anniversary of the PAH Hypothesis, ed. C Joblin & A. G. G. M. Tielens (Les Ulis: EDP Science), 177
Coustenis, A., Salama, A., Schulz, B., et al. 2003, Icar, 161, 383
Dohnálek, Z., Kimmel, G. A., & Ciolli, R. L. 2000, JChPh, 112, 5932
Fortes, A. D., & Capelli, S. C. 2018, PCCP, 20, 16736
Garozzo, M., Fulvio, D., Gomis, O., Palumbo, M. E., & Strazzulla, G. 2008, P&SS, 56, 1300
Gerakines, P. A., & Hudson, R. L. 2015a, ApJL, 805, L20
Gerakines, P. A., & Hudson, R. L. 2015b, ApJL, 808, L40
Gerakines, P. A., Yarnall, Y. Y., & Hudson, R. L. 2022, MNRAS, 509, 3515
Glover, D. E., & Hollenberg, J. L. 1969, JPhCh, 73, 889
Groner, P., Stolkin, I., & Günthard, H. H. 1973, JPhE, 6, 122
Herzberg, G. 1945, Molecular Spectra and Molecular Structure II. Infrared and Raman Spectra of Polyatomic Molecules (New York: Van Nostrand)
Hollenberg, J. L., & Dows, D. A. 1961, JChPh, 34, 1061

Hollenberg, J. L., & Dows, D. A. 1962, JChPh, 37, 1300
Hollenberg, J. L., & Glover, D. E. 1967, JPhCh, 71, 1544
Hornig, D. F., White, H. F., & Reding, F. P. 1958, SpecActa, 12, 338
Hudson, R. L. 2016, PCCP, 18, 25756
Hudson, R. L. 2020, Icar, 338, 113548
Hudson, R. L. 2022, Icar, 384, 115091
Hudson, R. L., Ferrante, R. F., & Moore, M. H. 2014a, Icar, 228, 276
Hudson, R. L., Gerakines, P. A., & Moore, M. H. 2014b, Icar, 243, 148
Hudson, R. L., Gerakines, P. A., & Yarnall, Y. Y. 2022b, ApJ, 925, 1
Hudson, R. L., Loeffler, M. J., & Gerakines, P. A. 2017, JChPh, 146, 0243304
Hudson, R. L., & Yarnall, Y. Y. 2022, Icar, 377, 114899
Hudson, R. L., Yarnall, Y. Y., & Gerakines, P. A. 2022a, PSJ, 3, 120
Imai, Y., Koiki, C., Chihara, H., et al. 2009, A&A, 507, 277
Ishii, K., Nakayama, H., Yoshida, T., Usui, H., & Koyama, K. 1996, Bull. Chem. Soc. Jpn., 69, 2831
Jacox, M. E. 1962, JChPh, 36, 140
Jakob, P., & Menzel, D. 1996, JChPh, 105, 3838
Jenniskens, P., & Blake, D. F. 1996, ApJ, 473, 1104
Kunde, V. G., Aikin, A. C., & Hanel, R. A. 1981, Natur, 292, 686
Luna, R., Molpeceres, G., Ortigoso, J., et al. 2018, A&A, 617, 1
Mair, R. D., & Hornig, D. F. 1949, JChPh, 17, 1236
May, R. A., Smith, R. S., & Kay, B. D. 2013, JPCA, 117, 11881
Mitchell, E. H., Raut, U., Teolis, B. D., & Baragiola, R. A. 2017, Icar, 285, 291
Mizuno, Y., Kofu, M., & Yamamuro, O. 2016, JPSJ, 86, 124602
Moore, M. H., Ferrante, R. F., Moore, W. J., & Hudson, R. L. 2010, ApJS, 191, 96
Moore, M. H., Hudson, R. L., & Carlson, R. W. 2007, Icar, 189, 409
Moore, M. H, Hudson, R. L, & Gerakines, P. A 2001, SpecActa, 57A, 843
Mouzay, J., Couturier-Tamburelli, I., Piétri, N., & Chiavassa, T. 2021, JGRE, 126, e06566
Mulliken, R. S. 1955, JChPh, 23, 1997
Mulliken, R. S. 1956, JChPh, 24, 1118
Nna-Mvondo, D., & Anderson, C. A. 2022, ApJ, 925, 1
Oliver, G. D., Eaton, M., & Huffman, H. M. 1948, JAChS, 70, 1502
Preuss, M., & Bechstedt, F. 2006, PhRvB, 73, 155413
Pryde, J. A., & Jones, G. O. 1952, Natur, 170, 685
Rao, C. N. R., & Rao, K. J. 1978, Phase Transitions in Solids (New York: McGraw Hill)
Ruiterkamp, R., Peeters, Z., Moore, M. H., & Ehrenfreund, P. 2005, A&A, 440, 391
Sato, K., Kurosawa, F., & Kammori, O. 1969, Bull. Japan. Chem. Soc., 42, 3593
Satorre, M. A., Millán, C., & Molpeceres, G. 2017, Icar, 296, 179
Schuhmann, M., Altwegg, K., Balsiger, H., et al. 2019, A&A, 630, A31
Sephton, M. A. 2002, NPRep, 19, 292
Smith, R. G., Robinson, G., Hyland, A. R., & Carpenter, G. L. 1994, MNRAS, 271, 481
Szczepaniak, K., & Person, W. B. 1972, AcSpe, 29A, 15
Takeda, T., Oguni, M., & Suga, H. 1990, Thermochim. Acta, 158, 195
Teanby, N. A., Irwin, P. G. J., & de Kok, R. 2009, Icar, 202, 620
Tempelmeyer, K. E., & Mills, D. W. 1968, JAP, 39, 2968
Tsuge, M., Nguyen, T., Oba, Y., Hama, T., & Kouchi, A. 2020, CPL, 760, 137999
Vinatier, S., Schmitt, B., Bézard, B., et al. 2018, Icar, 310, 89
Wang, H., Pring, A., Ngothai, Y., & O'Neill, B. 2005, GeCoA, 69, 415
Wood, B. E., & Roux, J. A. 1982, JOSA, 72, 720
Yamada, H., & Person, W. B. 1964, JChPh, 40, 309
Yarnall, Y. Y., Gerakines, P. A., & Hudson, R. L. 2020, MNRAS, 494, 4606
Yuan, H., Gibson, K. D., Killelea, D. R., & Sibener, S. J. 2013, SurSc, 609, 177